

# Synthesis of Shell Cross-Linked Micelles with pH-Responsive Cores Using ABC Triblock Copolymers

Shiyong Liu,\* Jonathan V. M. Weaver, Yiqing Tang, Norman C. Billingham, and Steven P. Armes\*

School of Chemistry, Physics and Environmental Science, University of Sussex, Brighton, East Sussex, BN1 9QJ, UK

Kevin Tribe

Polymer Laboratories, Essex Road, Church Stretton, Shropshire, SY6 6AX, UK

Received March 21, 2002; Revised Manuscript Received May 28, 2002

**ABSTRACT:** A series of well-defined poly[(ethylene oxide)-*block*-2-(dimethylamino)ethyl methacrylate-*block*-2-(diethylamino) methacrylate] (PEO–DMA–DEA) triblocks were synthesized by successive ATRP polymerization of DMA and DEA monomers using PEO-based macroinitiators of different molecular weights. These triblock copolymers dissolved molecularly in aqueous solution at low pH; on addition of NaOH, micellization occurred at pH 7.1 to form three-layer “onionlike” micelles comprising DEA cores, DMA inner shells, and PEO coronas. Above pH 7.3, dynamic light scattering studies indicated unimodal, near-monodisperse populations, with mean micelle diameters of 27–84 nm depending on block compositions (for PEO<sub>113</sub> triblock copolymers) and polydispersities typically less than 0.10. The average hydrodynamic diameter ( $\langle D_h \rangle$ ) of the micelles decreased as the solution pH was increased from pH 7.3 to pH 9.0, indicating that the micelles become more compact due to deprotonation of the tertiary amine residues in the DMA and DEA blocks. <sup>1</sup>H NMR studies supported a three-layer micelle structure and also revealed changes in the hydrophilicity of the DMA chains in the inner shell during cross-linking, which was achieved by adding the bifunctional alkyl iodide, 1,2-bis(2-iodoethoxy)ethane (BIEE). Selective quaternization of the DMA residues by the BIEE leads to increased hydrophilicity and colloid stability for the shell cross-linked (SCL) micelles. The minimum amount of BIEE required to “lock-in” the micellar structure depended on the thickness of the PEO corona: shorter PEO chains led to enhanced cross-linking efficiency. At pH 8.5, the hydrodynamic diameter of un-cross-linked micelles increased rapidly above 40–50 °C due to the LCST behavior of the neutral DMA chains in the inner shell. In contrast, the dimensions of the SCL micelles in dilute aqueous solution are independent of temperature. These SCL micelles exhibit reversible swelling on varying the solution pH. At low pH, the DEA cores become protonated and hence hydrophilic. The effect of varying the block composition and the target degree of cross-linking on the structural stability and pH-dependent (de)swelling of the SCL micelles was systematically studied. Longer DEA blocks and lower target degrees of cross-linking led to increased swellability, as expected.

## Introduction

In 1996, Wooley and co-workers published the first paper on shell cross-linked (SCL) micelles.<sup>1</sup> Since that seminal work, there has been increasing interest in SCL micelles.<sup>2–4</sup> These fascinating supramolecular structures combine the properties of micelles, microgels, nanoparticles, and dendrimers, and various applications such as targeted drug delivery, sequestration of metabolites, and entrapment of environmental pollutants have been suggested. In particular, recent efforts have focused on the synthesis of SCL micelles that have either hollow cores<sup>5,6</sup> or tunably hydrophilic cores.<sup>7–9</sup> Both Wooley's group and Liu and co-workers have prepared hollow SCL micelles by selective chemical degradation of the core-forming block,<sup>5,6</sup> whereas SCL micelles with tunably hydrophilic cores have been synthesized either by the in situ deprotection of a hydrophobic core-forming block<sup>8,9</sup> or by using core-forming blocks which exhibit dual hydrophilic/hydrophobic character.<sup>7</sup> In principle, hollow SCL micelles offer larger loading capacities, but tunably hydrophilic cores

are attractive since no core removal step is required, and there is the potential for triggered release of encapsulated actives via different chemical stimuli (pH, temperature, ionic strength, etc.).

In 1998, we described the first example of synthesis of SCL micelles with tunable core hydrophilicity.<sup>7a</sup> An aqueous micellar solution of partially quaternized poly[2-(dimethylamino)ethyl methacrylate-*block*-2-(*N*-morpholino)ethyl methacrylate] (DMA–MEMA) was reacted with a bifunctional cross-linker, 1,2-bis(2-iodoethoxy)ethane (BIEE), in aqueous solution at 60 °C. Under these conditions the MEMA block is above its cloud point and forms the micelle core. On cooling to 20 °C, the hydrophobic MEMA micelle cores become hydrated. Thus, the SCL micelle cores could be reversibly (de)hydrated depending on the solution temperature.

One major drawback in the synthesis of conventional SCL micelles is that shell cross-linking must be carried out at high dilution (typically <0.50% solids) in order to avoid extensive intermicellar cross-linking. Unless this problem is addressed, it is unlikely that the synthesis of SCL micelles will be commercially viable, even for specialty applications. Fortunately, we have recently demonstrated that ABC triblock copolymers offer great advantages over conventional AB diblock

\* To whom correspondence should be addressed: Tel UK + 1273-678650; Fax UK + 1273-677196; e-mail S.P.Armes@sussex.ac.uk; S.Liu@sussex.ac.uk.

copolymers, since the former allow shell cross-linking to be carried out at high solids (>10% w/v) with little or no intermicellar cross-linking. An example of this is a PEO–DMA–MEMA triblock [PEO = poly(ethylene oxide)] prepared by oxyanion-initiated polymerization.<sup>10</sup> This triblock forms micelles with MEMA cores and PEO coronas in aqueous solution in the presence of salt and BIEE was used to selectively cross-link the DMA residues in the inner shell. Intermicellar cross-linking was negligible, because the coronal PEO chains ensured minimal interpenetration of the micelles due to steric stabilization. In view of this success, all of our current synthetic effort is now devoted to the synthesis of ABC triblock copolymers, rather than AB diblocks.

Given the stringent purification required for ionic polymerizations, increasing attention is being given to the use of atom transfer radical polymerization<sup>11</sup> (ATRP) for the preparation of the block copolymer precursors for SCL micelles.<sup>2d,e,8,9,12</sup> Our group has developed ATRP for the efficient polymerization of hydrophilic monomers in either water or alcoholic media at room temperature.<sup>13</sup> Recently, we have exploited aqueous ATRP in order to develop a one-pot, solventless synthesis of SCL micelles with thermoresponsive PPO cores at high solids.<sup>11</sup>

For some applications the solution pH is easier and more convenient to control than either temperature or salt concentration.<sup>14–17</sup> Moreover, pH-induced micellization can lead to more hydrophobic micelle cores than temperature-induced micellization.<sup>16d</sup>

Herein, we describe the efficient synthesis of SCL micelles with pH-responsive cores from poly[(ethylene oxide)-*block*-2-(dimethylamino)ethyl methacrylate-*block*-2-(diethylamino)ethyl methacrylate], [PEO–DMA–DEA], triblock copolymers prepared via ATRP. The pH-induced micellar self-assembly and the effect of subsequent shell cross-linking on the size and colloidal stability of the micelles are studied in detail. The effect of varying the relative block compositions and the target degree of inner-shell cross-linking on the pH-induced (de)swelling of the SCL micelles was also investigated.

## Experimental Section

**Materials.** 2-(Dimethylamino)ethyl methacrylate (DMA) and 2-(diethylamino)ethyl methacrylate (DEA) were obtained from Aldrich. These monomers were passed through basic alumina columns, then vacuum-distilled from CaH<sub>2</sub>, and stored at –20 °C prior to use. Copper(I) bromide (CuBr), 2,2'-bipyridine (bpy), 2-bromoisobutyl bromide, triethylamine, three monohydroxy-capped poly(ethylene oxides) with mean degrees of polymerization of 23, 45, and 113 (designated PEO<sub>23</sub>–OH, PEO<sub>45</sub>–OH, and PEO<sub>113</sub>–OH), and all other chemicals were purchased from Aldrich and used without further purification.

**Preparation of PEO Macroinitiator (1).** For a typical example, in a 500 mL three-neck flask, PEO<sub>113</sub>–OH (50.0 g, 0.01 mol) was dissolved in 250 mL of toluene. After azeotropic distillation of 30–40 mL of toluene at reduced pressure to remove traces of water, triethylamine (2.78 mL, 0.02 mol) was added, and the solution was cooled to 0 °C. 2-Bromoisobutyl bromide (2.47 mL, 0.02 mol) was added dropwise via syringe over 1 h, and the reaction mixture was stirred overnight at room temperature. The stirred solution was treated with charcoal, which was subsequently removed by filtration, and most of the toluene was removed by rotary evaporation prior to precipitation into a 10-fold excess of ether. The crude polymer was dried under vacuum, dissolved in water at pH 8–9, and then extracted with dichloromethane. The organic

layers were collected and dried over MgSO<sub>4</sub>, and removal of the solvent under vacuum afforded the purified macroinitiator. <sup>1</sup>H NMR studies in D<sub>2</sub>O ( $\delta = 1.84$  (6 H),  $\delta = 3.56$  (456 H)) indicated that the hydroxyl end group of the PEO<sub>113</sub>–OH was fully esterified.

**Preparation of PEO–DMA–DEA Triblock Copolymer.** Cu(I)Br and bpy were added to a round-bottomed flask equipped with a stir bar. This flask was then sealed with a rubber septum, evacuated and filled with dry nitrogen twice. The PEO macroinitiator was dissolved in water and degassed via two freeze–thaw cycles, and the solution was transferred into the reaction flask via a double-tipped needle. After stirring for a few minutes a light green, homogeneous solution was obtained. Degassed DMA monomer was then introduced into the flask via a double-tipped needle to produce a 50% v/v aqueous DMA solution and start the polymerization. The reaction solution turned dark brown and became progressively more viscous, indicating the onset of polymerization; an exotherm of about 5–10 °C was noted. To monitor the extent of polymerization of DMA (and also DEA, see below), aliquots were taken at regular intervals and assessed by <sup>1</sup>H NMR spectroscopy and THF GPC, respectively. After about 15 min, the conversion had reached about 98%. Degassed DEA monomer in methanol was then added via a double-tipped needle to make a methanol/water (2:1 v/v) mixture. The reaction mixture turned deeper brown within a few minutes of the addition of DEA, and a second exotherm of about 5–8 °C was observed. Addition of excess methanol containing CuBr<sub>2</sub> terminated the polymerization, as indicated by the rapid color change from brown to blue. The reaction solution was then passed through a silica gel column to remove the copper catalyst. After evaporating all the solvent, the solid was washed with excess *n*-hexane to remove residual DEA monomer. Drying in a vacuum oven at room temperature yielded colorless polymer. Final purification of the PEO–DMA–DEA triblock from unreacted PEO macroinitiator (or PEO–DMA diblock copolymer) was achieved by repeated aqueous extraction prior to characterization studies.

**Preparation of Micelles and SCL Micelles.** The PEO–DMA–DEA triblock copolymers were molecularly dissolved in water at pH 2.0 at different concentrations, and the solution pH was adjusted to pH 8–9 so as to induce micelle formation. Shell cross-linking was achieved by adding BIEE at pH 8.5–9.0 and stirring the solution for at least 3 days at room temperature. Target degrees of quaternization were calculated from the [BIEE]/[DMA] molar ratio, allowing for the bifunctionality of the BIEE reagent. The actual degree of cross-linking cannot be easily obtained experimentally, but the degree of quaternization can be estimated using <sup>1</sup>H NMR spectroscopy (see later).

**Characterization.** Molecular weights and molecular weight distributions were measured by THF GPC (one PLgel 3  $\mu$ m MIXED-E 300  $\times$  7.5 mm column), THF eluent, PMMA calibration standards, and a refractive index detector.

Dynamic light scattering (DLS) studies were performed on a Brookhaven Instruments Corp. BI-200SM goniometer equipped with a BI-9000AT digital correlator using a solid-state laser (125 mW,  $\lambda = 532$  nm) at a fixed scattering angle of 90°. The intensity-average hydrodynamic diameters,  $\langle D_h \rangle$ , and polydispersities of the micelles were obtained by cumulants analysis of the experimental correlation function.<sup>18,19</sup>

Static light scattering studies were performed using a Wyatt Instruments DAWN DSP laser photometer, equipped with a 5 mW He–Ne laser ( $\lambda = 632.8$  nm) and 18 photodiode detectors at scattering angles ranging from 22.5° to 147°. In static light scattering, the angular dependence of the excess absolute time-averaged scattered light intensity, known as the Rayleigh ratio  $R_{v,v}(q)$ , of dilute polymer solutions allows the apparent weight-average molar mass ( $M_w$ )<sub>app</sub> and the root-mean-square  $z$ -average radius of gyration  $\langle R_g^2 \rangle_z^{1/2}$  (or written as  $\langle R_g \rangle$ ) to be calculated via a Zimm plot, where  $q$  is the scattering vector. The  $dn/dc$  values of the micellar solutions were measured at 20 °C using an Optilab DSP interferometric refractometer ( $\lambda = 633$  nm).

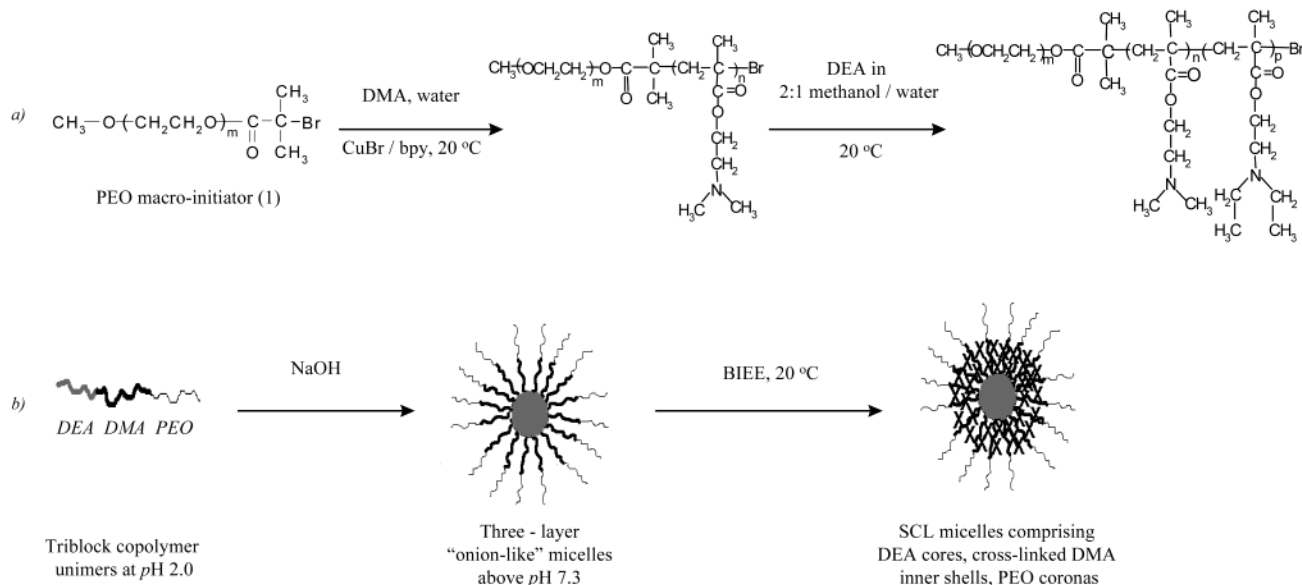


**Figure 1.** (a) Reaction scheme for the syntheses of PEO–DMA–DEA triblock copolymers. (b) Schematic illustration of the formation of three-layer “onion” micelles and shell cross-linked micelles from PEO–DMA–DEA triblock copolymers.

The particle size distributions of the SCL micelles were also assessed using a Polymer Laboratories particle size distribution analyzer (PL-PSDA). This instrument uses the principle of packed column hydrodynamic chromatography (HDC) to fractionate particles according to their hydrodynamic volume. Hence the technique is similar to GPC, except that the packed bed comprises nonporous beads and separation takes place in the channels between the beads. HDC is a relative technique, and the conversion from elution time to particle size involves using a series of near-monodisperse polystyrene latexes (e.g. Duke Scientific) as calibration standards. A type I cartridge, with a nominal operating range of 5–300 nm, was selected, and the eluent flow rate was 2.0 mL min<sup>-1</sup>. Shell cross-linked micellar solutions of either 2.0 or 2.5% w/v at pH 3 or 10 were filtered through a 2 μm Whatman filter prior to analysis, and the injection volume was 20 μL.

Electrophoresis measurements were carried out using a Malvern ZetaMasterS instrument. Zeta potentials were calculated from mobilities using the Henry equation and determined as a function of solution pH (0.01 M NaCl, 25 °C).

All <sup>1</sup>H NMR spectra were recorded on 1.0% w/v copolymer solutions in either D<sub>2</sub>O or *d*<sub>6</sub>-2-propanol using a Bruker Avance DPX 300 MHz spectrometer.

## Results and Discussion

**Synthesis of PEO–DMA–DEA Triblock Copolymers.** Zeng et al. recently described the aqueous ATRP of DMA, which was reported to be sensitive to the type of initiator, ligand, and catalyst employed.<sup>20</sup> When CuBr/bpy was used as catalyst in combination with methyl α-bromophenylacetate (MBP) as initiator, first-order kinetics and a linear increase in the number-average molecular weight with monomer conversion was achieved, indicating good living character. However, there was some evidence that polydispersities increased with conversion ( $M_w/M_n = 1.30$  at 85% conversion but  $M_w/M_n = 1.5$  at 95% conversion). Our group has also studied the polymerization of DMA in aqueous media, typically using PEO-based macroinitiators.<sup>21</sup> A very fast polymerization was observed (more than 95% conversion within 15 min). The number-average molecular weight measured by GPC increased linearly with conversion, although the semilogarithmic conversion plot was linear only up to 40% conversion. The kinetic details of the polymerization of DMA by ATRP will be published elsewhere.<sup>22</sup>

In principle, there are two possible synthetic routes to obtain PEO–DMA–DEA triblock copolymer. The first approach is to terminate the polymerization of DMA, purify the resulting PEO–DMA diblock copolymer and use this as a macroinitiator. The second approach is a “one-pot” synthesis via sequential monomer addition (see Figure 1). Our attempts to use the first method were unsuccessful; the PEO–DMA macroinitiator (purified by passing through a neutral alumina or silica gel column and then isolated by precipitation into *n*-hexane) either did not initiate DEA polymerization at all, or only very low conversions were obtained. Other workers have reported similar problems of chain-end deactivation, which may involve internal displacement of the terminal halogen atom by its neighboring tertiary amine group.<sup>11e,23</sup>

The second approach is considered to be somewhat problematic with conventional ATRP conducted in organic solvents; it is generally believed that it is unwise to allow the first monomer to proceed to very high conversion (above, say, 90%) because termination becomes much more likely under monomer-starved conditions.<sup>24</sup> Fortunately, this does not appear to be the case for the polymerization of various hydrophilic methacrylates in protic media.<sup>25–28</sup> DEA monomer is not water-miscible, so methanol is required as a cosolvent. After the polymerization of the DMA block using the PEO macroinitiator had reached 98% conversion, DEA monomer in methanol was added to make a methanol/water (2/1 v/v) mixture, and the polymerization continued, as evidenced by a second exotherm.

Figure 2 shows the typical evolution of GPC chromatograms during the syntheses of PEO–DMA–DEA triblock copolymers using a PEO<sub>113</sub>–Br macroinitiator. The target degrees of polymerization (DP) were 30 and 50 for the DMA and DEA blocks, respectively. Chromatogram 2 shows the GPC trace of the PEO–DMA diblock copolymer just before the addition of DEA; the polymerization of the DMA was almost complete at this point (98% conversion). A shoulder corresponding to unreacted PEO<sub>113</sub> macroinitiator is evident. Curve-fitting (using the known half-width of the peak obtained for pure PEO macroinitiator) allowed a PEO macroinitiator efficiency of around 80% to be estimated. Much

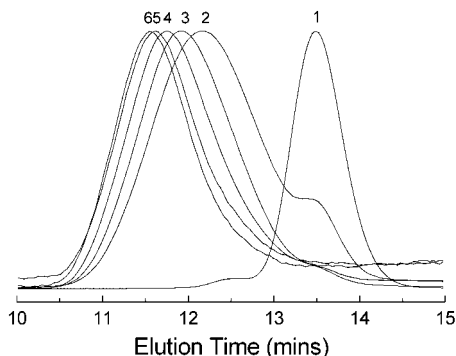


**Figure 2.** Evolution of GPC chromatograms during the syntheses of PEO–DMA–DEA triblock copolymers with a target degree of polymerization of 30 and 50 for DMA and DEA blocks, respectively, using PEO<sub>113</sub>–Br initiator and PEO<sub>113</sub>–Br:CuBr:bpy = 1:1:2: (1) PEO<sub>113</sub>–Br macroinitiator; (2) 15 min after the polymerization of DMA block in water, just before the addition of DEA monomer in methanol to make a methanol/water (2/1 v/v) mixture; (3) 12 min after addition of DEA monomer; (4) 20 min after addition of DEA; (5) 40 min after addition of DEA; (6) 75 min after addition of DEA.

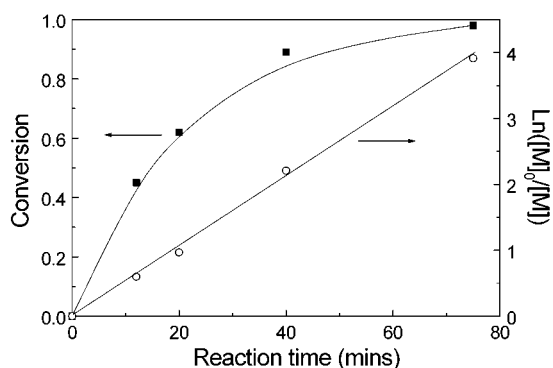


**Figure 3.** Kinetic plot for the ATRP of DEA block at 20 °C. The reaction conditions are the same as those stated in Figure 2.

higher initiator efficiencies (>95%) were obtained with the PEO<sub>23</sub>–Br macroinitiator.

The GPC chromatograms in Figure 2 indicated a continuous increase in molecular weight during the polymerization of DEA. It is also noteworthy that the shoulder that corresponds to the residual PEO macroinitiator continued to decrease in intensity and finally disappeared after 89% conversion of the DEA. At this point in the polymerization, the residual PEO impurity comprises less than 5% by mass of the total copolymer present, which is close to the GPC detection limit. It should be noted that chromatograms 5 and 6 (for which the DEA conversions are 89% and 96%, respectively) are monomodal, and there is little evidence of tailing to low molecular weight, indicating that premature termination at the end of the DMA polymerization is minimal.

On the basis of the GPC results and conversions calculated from concomitant <sup>1</sup>H NMR studies, we studied the kinetics of polymerization for the DEA block. Figure 3 depicts the kinetic data for the polymerization of DEA: a conversion of 96% was obtained within 75 min; the linear increase of ln([M]<sub>0</sub>/[M]) vs time indicates that this reaction is first order with respect to DEA and that the concentration of active species remains essentially constant throughout this second-stage polymerization. The GPC results shown in Figure 4 indicate that the number-average molecular weight increased

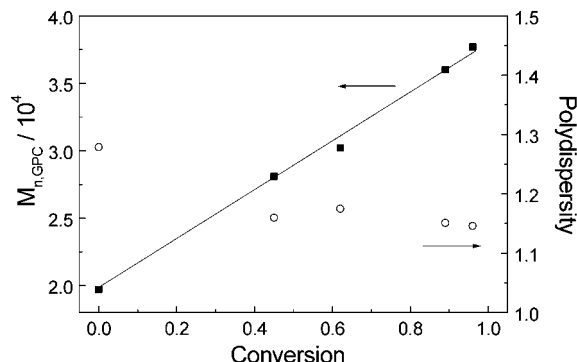


**Figure 4.** Evolution of molecular weight and polydispersity with conversion for polymerization of the DEA block via ATRP. The experimental conditions are the same as those described in Figure 2.

linearly with conversion. This result, together with a relatively narrow molecular weight distribution ( $M_w/M_n$  decreased gradually from 1.28 just before the addition of DEA to 1.14 at a DEA conversion of 96%), indicates that the polymerization is relatively well controlled. We and others have already shown that alcohol/water mixtures are preferred media for the controlled ATRP of various methacrylates such as 2-hydroxyethyl methacrylate,<sup>26</sup> glycerol monomethacrylate,<sup>27</sup> 2-hydroxypropyl methacrylate,<sup>27</sup> 2-methacryloyloxyethylphosphorylcholine,<sup>28</sup> and *n*-butyl methacrylate.<sup>29</sup> It appears that DEA can be added to this growing list.

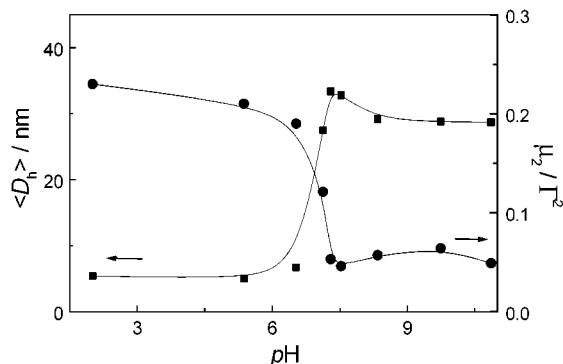
Further purification of the triblock copolymer was achieved by washing it with excess *n*-hexane to remove residual DEA monomer. After drying in a vacuum oven at room temperature, the triblock copolymer was extracted with water several times to remove any unreacted PEO macroinitiator or PEO–DMA diblock copolymer. PEO macroinitiators with number-average molecular weights of approximately 1000, 2000, and 5000 were used to prepare a series of PEO–DMA–DEA triblock copolymers with different DEA block lengths, while keeping the cross-linkable DMA block length essentially unchanged. The final block compositions were calculated from <sup>1</sup>H NMR spectra. Table 1 lists the molecular parameters of triblock copolymers synthesized in this study, together with the  $M_n$  values and polydispersity data obtained from GPC.

**pH-Induced Formation of Three-Layer “Onion” Micelles.** The DMA and DEA homopolymers are both weak polybases with  $pK_a$ 's of about 7.0 and 7.3, respectively.<sup>16</sup> At room temperature, DMA homopolymer is water-soluble over a wide pH range. However, it exhibits inverse temperature solubility behavior and precipitates from neutral or basic aqueous solution between 32 and 53 °C, depending on its molecular weight. In contrast, DEA homopolymer is water-insoluble at neutral or alkaline pH. Below pH 7.0, it is soluble as a weak cationic polyelectrolyte due to protonation of the tertiary amine groups.

Our group has previously synthesized DMA–DEA diblock copolymers via group transfer polymerization. These diblock copolymers dissolve molecularly in acidic media, but at pH 7–8, they form micelles with hydrophobic DEA cores and neutral (or only weakly cationic) DMA coronas due to deprotonation of both blocks. At higher pH, the micelles aggregate and precipitate.<sup>16</sup> Using PEO–DMA–DEA triblock copolymers instead of DMA–DEA diblock copolymers should increase the micelle stability in alkaline media due to

**Table 1. Molecular Parameters of PEG–DMA–DEA Triblock Copolymers Synthesized in This Study**

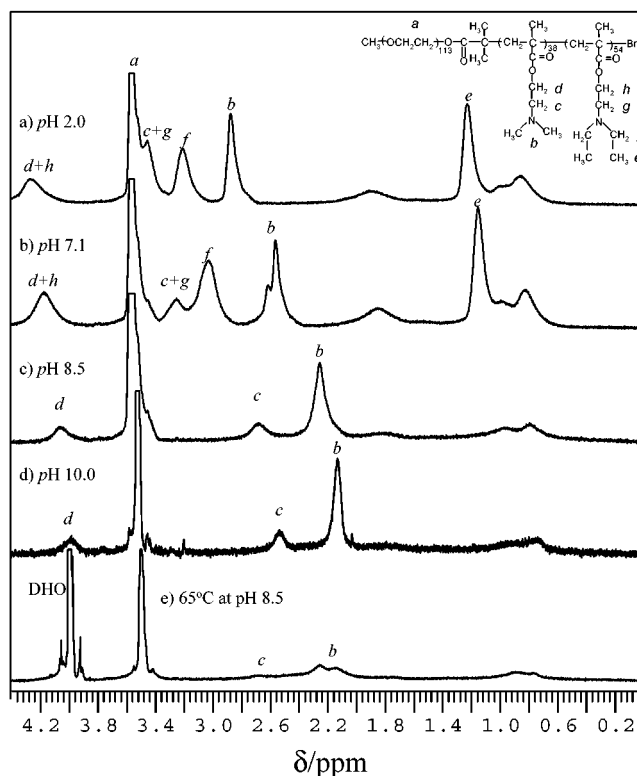
sample code	DP of PEG block	DP of DMA block	DP of DEA block	DEA content (mol %)	$M_{n,GPC}$	$M_w/M_n$
PEG <sub>113</sub> –DMA <sub>38</sub> –DEA <sub>44</sub>	113	38	44	23	28 100	1.19
PEG <sub>113</sub> –DMA <sub>38</sub> –DEA <sub>54</sub>	113	38	54	26	33 100	1.20
PEG <sub>113</sub> –DMA <sub>38</sub> –DEA <sub>86</sub>	113	38	86	36	35 900	1.19
PEG <sub>113</sub> –DMA <sub>38</sub> –DEA <sub>125</sub>	113	38	125	45	38 900	1.34
PEG <sub>45</sub> –DMA <sub>41</sub> –DEA <sub>40</sub>	45	41	40	32	26 200	1.23
PEG <sub>45</sub> –DMA <sub>40</sub> –DEA <sub>81</sub>	45	40	81	49	32 200	1.30
PEG <sub>23</sub> –DMA <sub>39</sub> –DEA <sub>40</sub>	23	39	40	39	23 900	1.35

**Figure 5.** Variation of intensity-average hydrodynamic diameter ( $\langle D_h \rangle$ ) and polydispersity  $\mu_2/\Gamma^2$  with pH for the PEO<sub>113</sub>–DMA<sub>38</sub>–DEA<sub>54</sub> triblock copolymer at 0.50% w/v in water.

the steric stabilization imparted by the hydrophilic PEO block.

Figure 5 shows the dynamic light scattering (DLS) results for a PEO<sub>113</sub>–DMA<sub>38</sub>–DEA<sub>54</sub> triblock copolymer at 0.50 wt % concentration. Below pH 7.0, this triblock copolymer is molecularly dissolved, with an intensity-average hydrodynamic diameter ( $\langle D_h \rangle$ ) of approximately 6–7 nm and very low scattering intensity. On addition of NaOH, micellization occurred above pH 7.1, as indicated by the bluish color that is characteristic of micellar solutions. Between pH 7.1 and 7.3, micellization is not complete: dynamic light scattering revealed two populations at 8 and 35 nm, corresponding to dissolved chains (unimers) and micelles, respectively. At pH 7.3 or higher, DLS only revealed one population corresponding to micelles. On the basis of chemical intuition, these micelles are expected to have a three-layer “onion” structure, with the DEA block occupying the micelle core and the DMA and PEO blocks forming the inner shell and corona, respectively. The  $\langle D_h \rangle$  of the micelles decreased from 33 to 29 nm as the solution pH was further increased from 7.3 to 8.5; i.e., the micelles became more compact due to further deprotonation of the DMA and DEA chains. On visual inspection the bluish color of the micellar solution becomes more intense. Above pH 8.5, the micelle size does not change significantly, and the aqueous micellar solutions remain colloidally stable over many months. Such micelles are near-monodisperse, with polydispersities typically less than 0.10.

Figure 6 shows the NMR spectra recorded for PEO<sub>113</sub>–DMA<sub>38</sub>–DEA<sub>44</sub> triblock copolymers at different pH. At pH 2 the copolymer chains are fully solvated, and all the signals expected for each block are visible. At pH 7.1, the DEA signals at  $\delta$  1.3 are still evident, indicating that this block is still hydrophilic, and DEA-core micelles are not yet formed (note also that progressive protonation causes a gradual shift in the signals due to the DMA and DEA residues). Actually, on the basis of the known  $pK_a$  values of DMA and DEA homopolymers,

**Figure 6.** <sup>1</sup>H NMR spectra recorded for the PEO<sub>113</sub>–DMA<sub>38</sub>–DEA<sub>44</sub> triblock copolymer at 1.0% w/v in D<sub>2</sub>O: (a) pH 2.0; (b) pH 7.1; (c) pH 8.5; (d) pH 10.0; (e) 65 °C at pH 8.5.

the degrees of protonation of the DMA and DEA blocks at pH 7.1 can be estimated to be 44% and 63%, respectively. Above pH 7.3, DLS indicates the onset of micellization. At pH 8.5, the signals due to the DEA block at  $\delta$  1.3 have completely disappeared, indicating the formation of relatively compact, hydrophobic DEA-core micelles.

In more alkaline media (pH 10), the DMA signals at  $\delta$  2.1 and  $\delta$  2.5 are also attenuated; comparison of the DMA signals at  $\delta$  2.5 to that of the PEO signal at  $\delta$  3.5 indicated a 26% decrease in relative intensity for the former signal. This indicates that partial desolvation of the hydrophilic DMA chains in the inner-shell occurs at higher pH.<sup>11</sup>

Table 2 summarizes DLS studies of the micelles obtained from a series of PEO–DMA–DEA triblock copolymers with different PEO and DEA chain lengths and an approximately constant DMA chain length. As the  $D_p$  of the DEA block was increased from 44 to 125, the micelle diameter increased from 27 to 84 nm (compare entries 1 and 4). It is well documented that larger micelles are invariably obtained when the chain length of the core-forming block is increased.<sup>16c</sup>

For the PEO<sub>45</sub>–DMA<sub>41</sub>–DEA<sub>40</sub> triblock copolymer (entry 5), much larger micelles with a  $\langle D_h \rangle$  of 60 nm were obtained compared to those from PEO<sub>113</sub>–DMA<sub>38</sub>–

**Table 2. A Summary of the Hydrodynamic Diameters and Solubilities for a Series of PEO–DMA–DEA Triblock Copolymers at 20 °C**

sample code	DEA content (mol %)	solution pH	micelle diameter <sup>a</sup>	PD <sup>a</sup>	aqueous solubility <sup>b</sup>
PEO <sub>113</sub> –DMA <sub>38</sub> –DEA <sub>44</sub>	23	9.4	27	0.068	yes
PEO <sub>113</sub> –DMA <sub>38</sub> –DEA <sub>54</sub>	26	10	29	0.029	slow
PEO <sub>113</sub> –DMA <sub>38</sub> –DEA <sub>86</sub>	36	9.3	37	0.091	no
PEO <sub>113</sub> –DMA <sub>38</sub> –DEA <sub>125</sub>	45	9.4	84	0.118	no
PEO <sub>45</sub> –DMA <sub>41</sub> –DEA <sub>40</sub>	32	10	60	0.172	no
PEO <sub>45</sub> –DMA <sub>40</sub> –DEA <sub>81</sub>	49	9.4	291	0.241	no
PEO <sub>23</sub> –DMA <sub>39</sub> –DEA <sub>40</sub>	39	9.5	248	0.265	no

<sup>a</sup> As determined by dynamic light scattering at 20 °C on 0.5% w/v solution. <sup>b</sup> Dissolution attempted in deionized water at 20 °C.

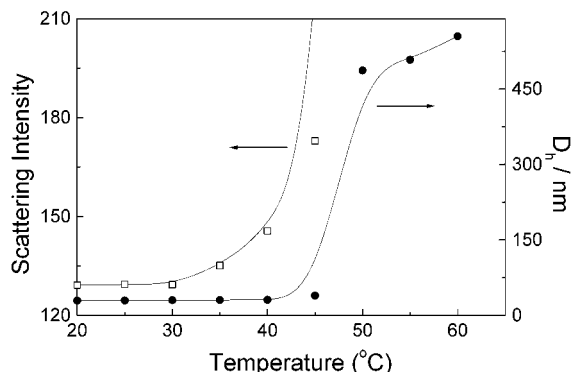


**Figure 7.** Variation of scattering intensity and  $\langle D_h \rangle$  as a function of temperature for PEO<sub>113</sub>–DMA<sub>38</sub>–DEA<sub>54</sub> triblock copolymer micelles at 0.50% w/v and pH 8.5 in water.

DEA<sub>44</sub> triblock copolymer (entry 1) with similar DMA and DEA chain length but different PEO chain length. In contrast, PEO<sub>45</sub>–DMA<sub>40</sub>–DEA<sub>81</sub> and PEO<sub>23</sub>–DMA<sub>39</sub>–DEA<sub>40</sub> triblock copolymers formed nonmicellar aggregates of 200–300 nm diameter. For these latter triblocks it should be noted that the dimensions of the colloidal aggregates decreased dramatically with copolymer concentration prior to micelle formation. For example, the aggregates formed by the PEO<sub>23</sub>–DMA<sub>39</sub>–DEA<sub>40</sub> triblock decreased from 248 nm at 0.50% w/v to 106 nm at 0.05% w/v. In contrast, the size of the micelles formed by the PEO<sub>113</sub>–DMA<sub>38</sub>–DEA<sub>44</sub> triblock copolymer varied by about 4 nm over the same concentration range.

The temperature stability of these “onion” micelles is also worth considering. In general, an ABC triblock copolymer dissolved in a suitable selective solvent will form three-layer “onion” micelles, with the insoluble C block occupying the core, the B block in the inner shell and the A block located in the corona. Then, if the solvency were tuned so as to desolvate the B block, some internal reorganization should occur, leading to micelles with cores comprising both the B and C blocks (which may be either nanophase-separated or intimately mixed), stabilized by the coronal A blocks. Higher aggregation numbers might be expected for these new micelles, since the hydrophilic/hydrophobic balance of the ABC triblock has been changed significantly. This hypothesis appears to be confirmed for the present triblock copolymer system in aqueous solution. Figure 7 shows the evolution of scattering intensity and  $\langle D_h \rangle$  as a function of temperature for the PEO<sub>113</sub>–DMA<sub>38</sub>–DEA<sub>54</sub> triblock at 0.50% w/v and pH 8.50. Below 45 °C the micelle size shows little change, although the scattering intensity increased gradually from 30 to 45 °C. Above 45 °C, the scattering intensity increased abruptly, accompanied by a dramatic increase in the aggregate size from 30 to about 400–500 nm diameter. At around this tempera-

ture the DMA block approaches its cloud point and becomes hydrophobic; presumably, the changing hydrophilic–hydrophobic balance leads to micellar fusion. Spectrum e shown in Figure 6 supports this hypothesis: the intensities of the signals due to the DMA residues at  $\delta$  2.1 and  $\delta$  2.5 are attenuated considerably, although they remain visible.

**Shell Cross-Linked Micelles with pH-Responsive Cores.** Shell cross-linked micelles were prepared by adding 1,2-bis(2-iodoethoxy)ethane (BIEE) to the micellar solution. BIEE reacts selectively with the DMA residues on adjacent block copolymer chains to “lock in” the micellar structure.<sup>7,10</sup> BIEE has relatively low water solubility and was initially dispersed as droplets. After 30 min, these droplets disappeared to form a homogeneous solution; this reaction solution was stirred at pH 8.5–9.0 for 3 days at room temperature.

The addition of BIEE led to the quaternization of DMA residues and hence cross-linking of the inner shell of the “onion” micelles. Typical <sup>1</sup>H NMR spectra of micellar solutions of PEO<sub>113</sub>–DMA<sub>38</sub>–DEA<sub>44</sub> with different target degrees of quaternization are shown in Figure 8.<sup>30</sup> The signals due to DMA residues at  $\delta$  2.1 and  $\delta$  2.5 decreased progressively with increasing target degree of cross-linking, and a new signal assigned to quaternized DMA units<sup>7,10</sup> appeared at  $\delta$  3.1. Comparing the integral of the  $\delta$  2.1 signal due to unquaternized DMA residues to that of the PEG block at  $\delta$  3.5 allows the actual degree of quaternization to be estimated (see Figure 9). The actual degree of quaternization increases monotonically with the target degree of quaternization as expected,<sup>30</sup> but the former is always significantly less than the latter. This is understandable, because some hydrolysis of the iodoethyl groups of the BIEE may well occur in aqueous solution, which would necessarily reduce the actual degree of cross-linking that is achieved. It is interesting to note that Wooley and co-workers were unable to monitor the extent of cross-linking by <sup>1</sup>H NMR spectroscopy because, in their case, the cross-linking chemistry led to *reduced* hydrophilicity of the cross-linked chains. However, quaternization of the DMA residues in our study leads to *increased* hydrophilicity, which allows the reaction to be conveniently monitored.

For SCL micelles prepared from 1.0% w/v aqueous solutions of PEO<sub>113</sub>–DMA<sub>38</sub>–DEA<sub>44</sub> in D<sub>2</sub>O, the solution pH was adjusted to pH 2 using DCl. If no shell cross-linking had occurred, dissociation into individual triblock copolymer chains would be expected, since the DEA core block becomes soluble under these conditions (as shown in Figure 5). However, provided that the target degree of quaternization was at least 35% (corresponding to actual degrees of quaternization of 20%), visual inspection confirmed the continued presence of Tyndall scattering characteristic of micellar solutions

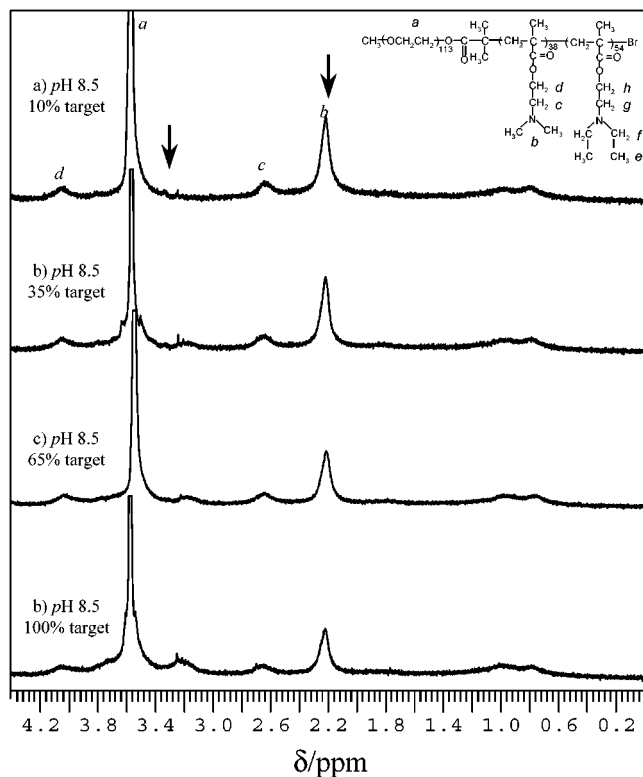


**Figure 8.**  $^1\text{H}$  NMR spectra of SCL micelles with different target degrees of cross-linking prepared from the  $\text{PEO}_{113}\text{-DMA}_{38}\text{-DEA}_{44}$  triblock copolymer at 1.0% w/v and pH 8.5 in  $\text{D}_2\text{O}$  at a target degree of cross-linking of (a) 10%, (b) 35%, (c) 65%, and (d) 100%.

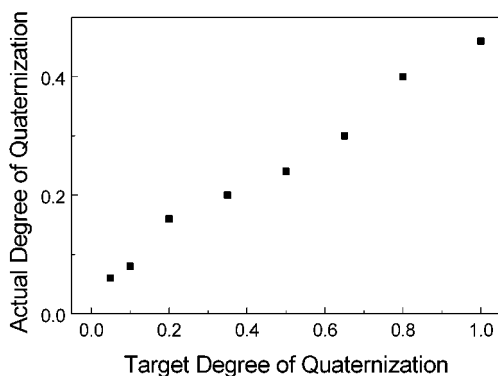


**Figure 9.** Relationship between the actual degree of quaternization vs target degree of cross-linking for SCL micelles prepared from  $\text{PEO}_{113}\text{-DMA}_{38}\text{-DEA}_{44}$  triblock copolymer at 1.0% w/v and pH 8.5 in  $\text{D}_2\text{O}$ .

and hence indicated successful covalent stabilization. DLS was used to examine all the SCL micelles. In addition to providing reliable particle size data, its increased sensitivity enabled the presence of SCL micelles to be confirmed at target degrees of quaternization lower than 35%; these results are summarized in Figure 10. Figure 10a shows the variation of scattering intensity due to SCL micelles at pH 9 and pH 2. The scattering intensity increases gradually with target degree of quaternization due to the introduction of BIEE, which leads to an increase in the micellar mass. At pH 2, the scattering intensity increased rapidly as the target degree of quaternization is increased from 5% to 35%. Above 35%, there is little change in the scattering intensity, indicating that the covalent stabilization of the micelles is complete.

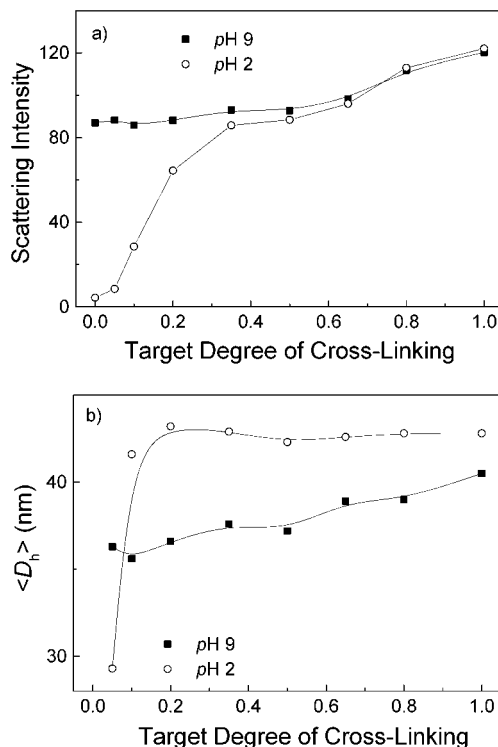


**Figure 10.** Variation in  $\langle D_h \rangle$  and scattering intensity with target degree of cross-linking for SCL micelles prepared from the  $\text{PEO}_{113}\text{-DMA}_{38}\text{-DEA}_{44}$  triblock copolymer at pH 9 and pH 2.

Figure 10b shows the dependence of  $\langle D_h \rangle$  of the SCL micelles at pH 10 and pH 2 on the target degree of cross-linking. Before cross-linking, the  $\text{PEO}_{113}\text{-DMA}_{38}\text{-DEA}_{44}$  micelles in  $\text{D}_2\text{O}$  have a hydrodynamic diameter of 35 nm. At a target degree of quaternization of 5%, the  $\langle D_h \rangle$  observed at pH 10 is larger than that at pH 2. This suggests that covalent stabilization of the SCL micelles is not complete under these conditions; this hypothesis is supported by the very low scattering intensity at pH 2 shown in Figure 10a. Examination of Figure 10a,b indicates that a minimum target degree of quaternization of 10% is required for the efficient preparation of SCL micelles using the  $\text{PEO}_{113}\text{-DMA}_{38}\text{-DEA}_{44}$  triblock copolymer under the stated conditions. The  $\langle D_h \rangle$  of successfully prepared SCL micelles at pH 2 is larger than that at pH 10 because the DEA chains in the core become hydrophilic at low pH due to protonation. In addition, protonation of unquaternized DMA residues in the inner layer will also lead to swelling. We cannot rule out the possibility that the protonated, cationic DEA chains may (partly) migrate through the cross-linked DMA layer and form a "mixed" corona with the hydrophilic PEO chains. Reduced swelling at low pH is observed at higher target degrees of cross-linking, as expected. Similar observations have been made by various groups for other SCL micelles.<sup>8,9,12</sup>

The aqueous electrophoresis data obtained for SCL micelles derived from the  $\text{PEO}_{113}\text{-DMA}_{38}\text{-DEA}_{86}$  and  $\text{PEO}_{45}\text{-DMA}_{41}\text{-DEA}_{40}$  triblock copolymers are summarized in Figure 11. The  $\zeta$  potentials for the latter SCL micelles are systematically larger than those of the former. This undoubtedly reflects the differing coronal layer thicknesses, since the longer PEO chains is expected to shield the cationic charge density more effectively. The  $\zeta$  potentials remain positive over the whole pH range due to the introduction of permanent

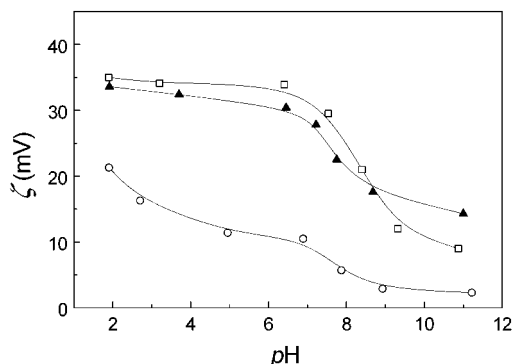


**Figure 11.** Variation of  $\zeta$  potential with pH for dilute (0.1 g/L) aqueous solutions of SCL micelles prepared from (▲) PEO<sub>45</sub>-DMA<sub>41</sub>-DEA<sub>40</sub> with a target degree of cross-linking of 100%, (□) PEO<sub>45</sub>-DMA<sub>41</sub>-DEA<sub>40</sub> with a target degree of cross-linking of 20%, and (○) PEO<sub>113</sub>-DMA<sub>38</sub>-DEA<sub>86</sub> with a target degree of cross-linking of 100%.

cationic charge during cross-linking. Below pH 7–8, which approximately corresponds to the  $pK_b$  of both types of tertiary amine units, the  $\zeta$  potential increased dramatically due to protonation of both the DEA block and also the unquaternized DMA residues in the inner shell; this is in agreement with the DLS results shown in Figure 10. It should also be noted that, for the PEO<sub>45</sub>-DMA<sub>41</sub>-DEA<sub>40</sub> triblock, slightly higher  $\zeta$  potentials are observed at the lower target degree of cross-linking (20%). It is suggested that this reduced degree of cross-linking allows the DEA chains more mobility; hence, a certain degree of intermixing of this block with the DMA chains, and possibly the coronal PEO chains, can occur.

The NMR spectra of SCL micelles prepared from a PEO<sub>113</sub>-DMA<sub>38</sub>-DEA<sub>44</sub> triblock with different target degrees of cross-linking at pH 2.0 are depicted in Figure 12. The reappearance of signals assigned to the DEA residues at low pH suggests that the SCL micelle cores become either hydrophilic or hollow, depending on the precise location of the DEA chains. At higher target degrees of cross-linking, resolution of the DEA signals is incomplete at low pH; presumably, the highly cross-linked DMA layer restricts the mobility of the DEA chains. It is even conceivable that the geometrically constrained DEA residues may become much less basic (less easily protonated) under these conditions.

The pH dependence of  $\langle D_h \rangle$  for SCL micelles derived from the PEO<sub>113</sub>-DMA<sub>38</sub>-DEA<sub>54</sub> triblock (target degree of cross-linking = 30%) is illustrated in Figure 13. Most of the size increase takes place at around physiological pH, which is consistent with the known  $pK_a$  values for the DMA and DEA blocks. Between pH 7 and pH 8 the micellar diameter increases from 34 to 47 nm, indicating an increase in the hydrodynamic volume by a factor of more than 2.6. This augurs well for the potential application of such SCL micelles as nanosized drug delivery vehicles since the abrupt change in hydrophilicity of the DEA cores (and concomitant increased permeability of the DMA cross-linked layer) should allow “triggered release” of hydrophobic drugs.

The temperature stability of an aqueous solution of SCL micelles prepared from the PEG<sub>113</sub>-DMA<sub>38</sub>-DEA<sub>54</sub> triblock (target cross-linking degree = 100%) is summarized in Figure 14. In contrast to the un-cross-linked micelles (see Figure 7), the scattering intensity and hydrodynamic diameter remain essentially unchanged from 20 to 80 °C. This is consistent with covalent

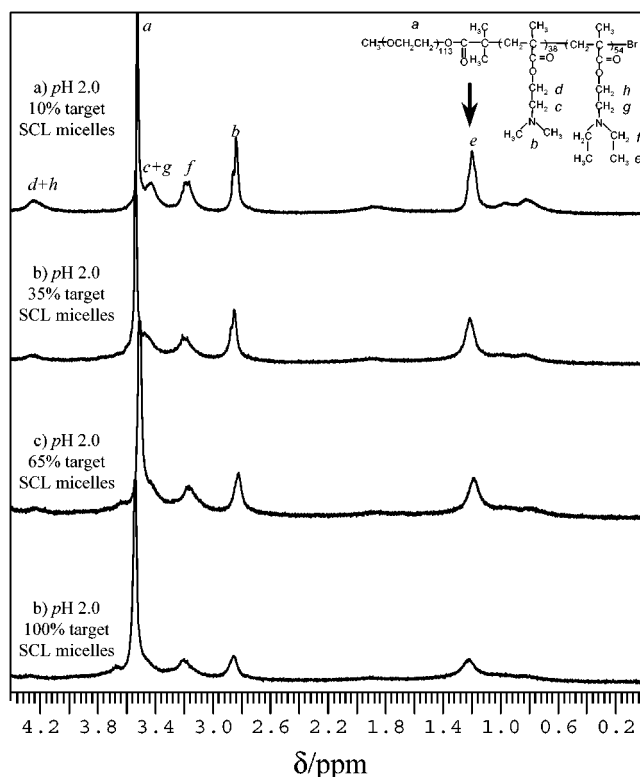


**Figure 12.** <sup>1</sup>H NMR spectra of SCL micelles prepared using the PEO<sub>113</sub>-DMA<sub>38</sub>-DEA<sub>44</sub> triblock copolymer at 1.0% w/v and pH 2 in D<sub>2</sub>O at the following target degrees of cross-linking: (a) 10%, (b) 35%, (c) 65%, and (d) 100%.

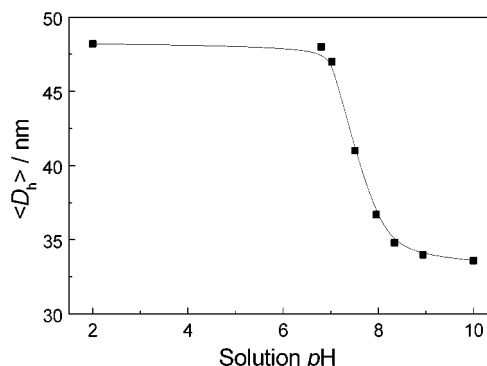


**Figure 13.** Variation of  $\langle D_h \rangle$  with solution pH for SCL micelles prepared from the PEO<sub>113</sub>-DMA<sub>38</sub>-DEA<sub>54</sub> triblock copolymer at 0.50% w/v with a target degree of cross-linking of 30%.

stabilization via quaternization, since this modification suppresses the inverse temperature solubility behavior of the DMA chains, rendering them permanently hydrophilic. Thus, the SCL micelles exhibit excellent colloid stability at elevated temperatures. Another interesting feature of these SCL micelles is that, although they are stable at pH 2, the addition of poly(methacrylic acid) (PMAA) leads to a white precipitate due to hydrogen-bonding-induced complexation<sup>31</sup> between the PMAA chains and the PEO corona of the SCL micelles. On the other hand, the addition of PMAA to the molecularly dissolved, un-cross-linked PEG<sub>113</sub>-DMA<sub>38</sub>-DEA<sub>54</sub> triblock at pH 2 led to a bluish solution with an intensity-average particle diameter of around 100 nm. Presumably, an inverted micellar morphology is obtained under these conditions, with a PMAA/PEO hydrogen-bonded core and the two protonated tertiary amine methacrylates forming the cationic corona. The



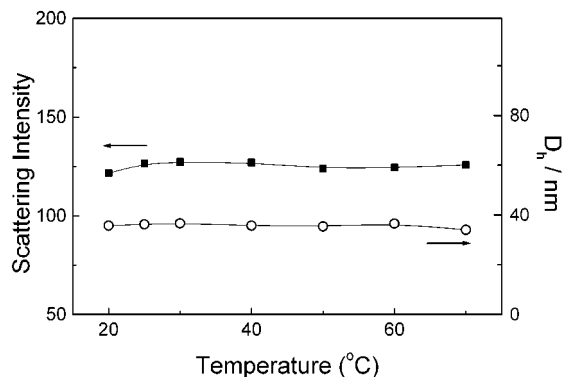


**Figure 14.** Variation of scattering intensity and  $\langle D_h \rangle$  as a function of temperature for SCL micelles prepared from the PEO<sub>113</sub>-DMA<sub>38</sub>-DEA<sub>54</sub> triblock copolymer at 0.50% w/v and pH 8.5 (the target degree of cross-linking was 100%).

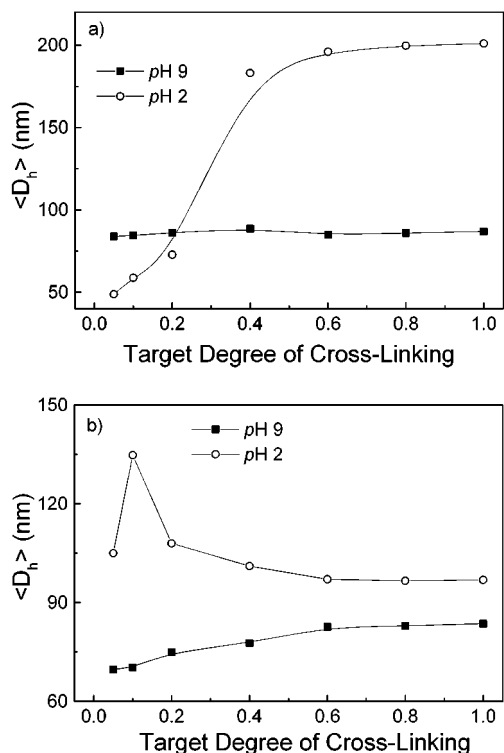


**Figure 15.** Variation in  $\langle D_h \rangle$  as a function of target degree of cross-linking at both pH 9 and pH 2 for SCL micelles prepared at 0.50% w/v from (a) the PEO<sub>113</sub>-DMA<sub>38</sub>-DEA<sub>125</sub> triblock copolymer and (b) the PEO<sub>45</sub>-DMA<sub>41</sub>-DEA<sub>40</sub> triblock copolymer.

above observations support the hypothesis that the PEO chains are located in the corona of the SCL micelles.

The variation in DLS diameter for SCL micelles derived from PEO<sub>113</sub>-DMA<sub>38</sub>-DEA<sub>125</sub> and PEO<sub>45</sub>-DMA<sub>41</sub>-DEA<sub>40</sub> triblocks at both pH 9 and pH 2 is depicted in Figure 15. For the PEO<sub>113</sub>-DMA<sub>38</sub>-DEA<sub>125</sub> triblock (Figure 15a), the minimum target degree of cross-linking must be greater than 40% for effective covalent stabilization of micelles. The diameter at pH 2 increased by a factor of almost 2.4 compared to that at pH 9, which corresponds to a volume increase of 13 times. In contrast, for the PEO<sub>45</sub>-DMA<sub>41</sub>-DEA<sub>40</sub> triblock it was found that a target degree of cross-linking of only 5% was sufficient to “lock in” the SCL micelle structure at pH 9 (see Figure 15b). For target degrees of cross-linking above 10% the degree of swelling achieved at pH 2 is progressively reduced. Comparing

these results to the data presented in Figure 10, it appears that triblocks with shorter PEO chains are more easily cross-linked and that the extent of swelling of the SCL micelles on changing the pH is more prominent. This suggests that increasing the size of the “headgroup” (in this case the PEO chains) leads to greater spatial separation between adjacent DMA chains within the micelles, which in turn reduces the efficiency of shell cross-linking. The results obtained from SCL micelles prepared using the PEO<sub>45</sub>-DMA<sub>40</sub>-DEA<sub>81</sub> triblock also suggest that longer DEA block lengths lead to increased swellability.

The dynamic and static light scattering data obtained for SCL micelles prepared from various PEO-DMA-DEA triblock copolymers at pH 9 and pH 2, respectively, are presented in Table 3. There are several noteworthy features. First, the SCL micelle aggregation number increases with (i) increasing DEA block length (for triblocks with the same PEO chain) and (ii) decreasing PEO chain length (for triblocks with similar DEA chain length). Second, for a target degree of cross-linking of 100%, the aggregation numbers obtained at pH 9 and pH 2 are similar within experimental error, indicating successful covalent stabilization of the micellar structures. Finally, for each SCL micelle, the radius of gyration  $\langle R_g \rangle$  at pH 9 is systematically lower than that at pH 2, confirming the swelling of the micelles due to protonation of DEA chains in the core. Moreover, the  $\langle R_g \rangle / \langle R_h \rangle$  ratio is always higher at pH 2 compared to that at pH 9. The  $\langle R_g \rangle / \langle R_h \rangle$  ratio at pH 9 is closer to the theoretical value of 0.774 for a uniform sphere, suggesting that the SCL micelles have a more extended conformation at pH 2. The micelle aggregation numbers for the last two entries are too high to be consistent with isolated, noninteracting spherical micelles with core-shell structures. We believe either that the micelles are weakly interacting or that ill-defined colloidal aggregates are formed. The former possibility is not unreasonable, because the PEO block is relatively short, and at pH 9 the DMA block is on the verge of becoming hydrophobic. Another possibility is that large, non-spherical colloidal structures such as lamellae, vesicles, or rods are formed under these conditions. TEM studies are in progress in order to distinguish between these possibilities.

One of the advantages of using an ABC triblock copolymer is that the shell cross-linking can be carried out at high copolymer concentration.<sup>10</sup> The synthesis of SCL micelles using the PEO<sub>113</sub>-DMA<sub>38</sub>-DEA<sub>44</sub> triblock was also attempted at 10% w/v with a target cross-linking degree of 50%. After cross-linking, DLS studies indicated a  $\langle D_h \rangle$  of 35 nm and a polydispersity of 0.071 at pH 9, with no evidence of any intermicellar cross-linking. At pH 2, the  $\langle D_h \rangle$  increased to 43 nm (polydispersity = 0.144). Thus, these SCL micelles can be prepared at relatively high solids, which is obviously attractive for potential commercial applications.

Finally, a new commercial particle size analyzer, the PSDA-PL (e.g. Polymer Laboratories), was used to assess the particle size distributions of SCL micelles prepared from the PEO<sub>113</sub>-DMA<sub>38</sub>-DEA<sub>54</sub> triblock copolymer at pH 10 and pH 3 (see Figure 16). At pH 10, the particle size ranged from 10 to 40 nm with a small tail extending to about 60 nm. The mean volume-average diameter was calculated to be 23 nm, which is much lower than the mean diameter obtained from DLS (33 nm). This is because the latter technique measures

**Table 3. A Summary of the Dynamic and Static Light Scattering Data for SCL Micelles from PEO–DMA–DEA Triblock Copolymers at 20 °C**

sample code	target degree of cross-linking (%)	solution pH	$\langle R_h \rangle$	$\langle R_g \rangle$	$M_w/10^6$	$N_{agg}^c$	$\langle R_g \rangle / \langle R_h \rangle$
PEO <sub>113</sub> –DMA <sub>38</sub> –DEA <sub>44</sub>	100 <sup>a</sup>	9.0	15	12	2.76	68	0.80
PEO <sub>113</sub> –DMA <sub>38</sub> –DEA <sub>44</sub>	100 <sup>a</sup>	2.0	17	15	2.81	69	0.88
PEO <sub>113</sub> –DMA <sub>38</sub> –DEA <sub>86</sub>	100 <sup>a</sup>	9.0	20	17	6.38	158	0.85
PEO <sub>113</sub> –DMA <sub>38</sub> –DEA <sub>86</sub>	100 <sup>a</sup>	2.0	22	31	6.88	170	1.41
PEO <sub>23</sub> –DMA <sub>39</sub> –DEA <sub>40</sub>	100 <sup>b</sup>	9.0	73	66	33.4	846	0.90
PEO <sub>23</sub> –DMA <sub>39</sub> –DEA <sub>40</sub>	100 <sup>b</sup>	2.0	75	88	39.7	1006	1.17

<sup>a</sup> SCL micelles prepared at 1.0% w/v solution at pH 9.0. <sup>b</sup> SCL micelles prepared at 0.1% w/v solution at pH 9.0. <sup>c</sup> Assuming that the target degree of cross-linking has been achieved.

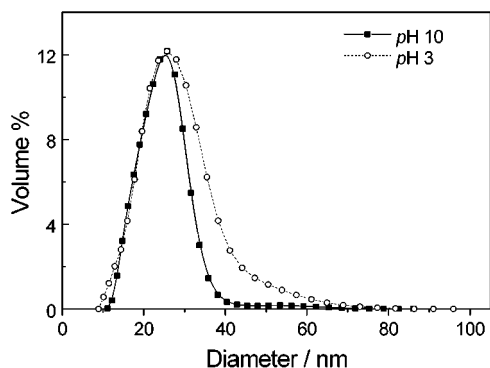


**Figure 16.** Typical volume-average particle size distributions at pH 10 and pH 3 obtained using the PL-PSDA instrument to analyze SCL micelles prepared from the PEO<sub>113</sub>–DMA<sub>38</sub>–DEA<sub>44</sub> triblock copolymer at 10.0% w/v copolymer concentration with a target degree of cross-linking of 50%.

an intensity-average diameter, which will always exceed the volume-average diameter. Assuming that the SCL micelles are spherical and have a log-normal distribution, a volume-average diameter of 25 nm can be computed from the DLS software, which is quite close to the value determined by the PSDA-PL technique. Figure 16 also shows the particle size distribution of the same SCL micelles at pH 3. The increase in volume-average particle diameter relative to that obtained at pH 10 again indicates swelling of the SCL micelles. As far as we are aware, this is the first time that the PSDA-PL technique has been applied to SCL micelles. Advantages of this sizing technique include (i) typical analysis times are less than 10 min, (ii) many samples can be run sequentially using the autosampler mode, (iii) the reported volume-average particle diameter is more likely to be comparable to that observed by electron microscopy, and (iv) no knowledge of the particle density is required. On the other hand, careful calibration is required, and as with DLS, solutions must be ultra-filtered prior to use. On balance, we believe that the PSDA-PL instrument is a useful new characterization tool for SCL micelles, and we intend to exploit this technique further in future studies.

**Conclusion.** In summary, a series of PEO–DMA–DEA triblock copolymers of variable block compositions were prepared by the sequential polymerization of DMA and DEA by ATRP using PEO macroinitiators. These triblock copolymers dissolved molecularly in aqueous solution at low pH; micellization occurred above pH 7.0 to form three-layer “onion” micelles with DEA cores, DMA inner shells, and PEO coronas. Above pH 7.3, dynamic light scattering (DLS) indicated a unimodal population of near-monodisperse micelles. The average hydrodynamic micelle diameter decreased as the solution pH was increased from 7.3 to 8.5, indicating that the micelles became more compact due to progressive

deprotonation of the DMA inner shell and DEA core. Efficient shell cross-linking of the triblock copolymers was achieved in aqueous solution at room temperature using 1,2-bis(2-iodoethoxy)ethane (BIEE) to selectively quaternize the DMA residues. It was found that the minimum amount of BIEE needed for covalent stabilization depends on the PEO block length, with less BIEE being required for shorter PEO chains. This is attributed to better micelle packing efficiencies and hence shorter separation distances between adjacent DMA chains within the inner shell. The SCL micelles exhibit enhanced colloid stabilities at elevated temperatures due to the increased hydrophilicity imparted by the quaternization/cross-linking chemistry. SCL micelles form insoluble complexes at low pH on addition of poly(methacrylic acid), which is consistent with the hypothesis that the PEO chains are located on the outside of the micelle, as expected. The DEA cores of the SCL micelles have tunable hydrophilicity depending on the solution pH. Reversible swelling is observed on lowering the solution pH from 9 to 2 due to protonation of the DEA chains in the micelle core. Most of this increase in size occurs at around pH 7–8, which corresponds approximately to the  $pK_b$ 's of the DMA and DEA residues. The block compositions and target degrees of cross-linking have a significant influence on the structural stability and pH-responsive (de)swelling of the SCL micelles. Longer DEA block lengths and lower target degrees of cross-linking lead to increased degrees of swelling for the SCL micelles.

**Acknowledgment.** EPSRC is acknowledged for postdoctoral grants to support S.L. (GR/N17409) and Y.T. (ROPA GR/R13784). J.V.M.W. acknowledges an EPSRC PhD studentship, and Laporte Performance Chemicals (Hythe, UK) is thanked for generous CASE support.

## References and Notes

- (1) (a) Thurmond, K. B.; Kowalewski, T.; Wooley, K. L. *J. Am. Chem. Soc.* **1996**, *118*, 7239. (b) Wooley, K. L. *J. Polym. Sci., Part A: Polym. Chem.* **2000**, *38*, 1397.
- (2) (a) Thurmond, K. B.; Kowalewski, T.; Wooley, K. L. *J. Am. Chem. Soc.* **1997**, *119*, 6656. (b) Huang, H.; Remsen, E. E.; Wooley, K. L. *Chem. Commun.* **1998**, 1415. (c) Huang, H.; Remsen, E. E.; Kowalewski, T.; Wooley, K. L. *J. Am. Chem. Soc.* **1999**, *121*, 3805. (d) Ma, Q.; Wooley, K. L. *J. Polym. Sci., Part A: Polym. Chem.* **2000**, *38*, 4805. (e) Becker, M. L.; Remsen, E. E.; Wooley, K. L. *J. Polym. Sci., Part A: Polym. Chem.* **2001**, *39*, 4152. (f) Ma, Q.; Remsen, E. E.; Kowalewski, T.; Wooley, K. L. *J. Am. Chem. Soc.* **2001**, *123*, 4627.
- (3) (a) Sanji, T.; Nakatsuka, Y.; Kitayama, F.; Sakurai, H. *Chem. Commun.* **1999**, 2201. (b) Sanji, T.; Nakatsuka, Y.; Ohnishi, S.; Sakurai, H. *Macromolecules*, **2000**, *33*, 8524.
- (4) Underhill, R. S.; Liu, G. *Chem. Mater.* **2000**, *12*, 2082.
- (5) (a) Huang, H.; Remsen, E. E.; Kowalewski, T.; Wooley, K. L. *J. Am. Chem. Soc.* **1999**, *121*, 3805. (b) Zhang, Q.; Remsen, E. E.; Wooley, K. L. *J. Am. Chem. Soc.* **2000**, *122*, 3642.

- (6) Ding, J.; Liu, J. *J. Phys. Chem. B* **1998**, *102*, 6107.
- (7) (a) Bütün, V.; Billingham, N. C.; Armes, S. P. *J. Am. Chem. Soc.* **1998**, *120*, 12135. (b) Bütün, V.; Lowe, A. B.; Billingham, N. C.; Armes, S. P. *J. Am. Chem. Soc.* **1999**, *121*, 4288.
- (8) Ma, Q.; Remsen, E. E.; Kowalewski, T.; Schaefer, J.; Wooley, K. L. *Nano Lett.* **2001**, *1*, 651–655.
- (9) Zhang, Z.; Liu, G.; Bell, S. *Macromolecules* **2000**, *33*, 7877.
- (10) Bütün, V.; Wang, X.-S.; de Paz Banez, M. V.; Robinson, K. L.; Billingham, N. C.; Armes, S. P. *Macromolecules* **2000**, *33*, 1.
- (11) (a) Wang, J. S.; Matyjaszewski, K. *J. Am. Chem. Soc.* **1995**, *117*, 5614. (b) Kato, M.; Kamagaito, M.; Sawamoto, M.; Higashimura, H. *Macromolecules* **1995**, *28*, 1721. (c) M Haddleton, D.; Waterson, C.; Derrick, P. J.; Jasieczek, C. B.; Shooter, A. J. *Chem. Commun.* **1997**, 683. (d) Patten, T. E.; Matyjaszewski, K. *Adv. Mater.* **1998**, *10*, 901. (e) Sawamoto, M.; Kamagaito, M. *Trends Polym. Sci.* **1996**, *4*, 371. (f) Matyjaszewski, K.; Xia, J. H. *Chem. Rev.* **2001**, *101*, 2921.
- (12) Liu, S.; Armes, S. P. *J. Am. Chem. Soc.* **2001**, *123*, 9910.
- (13) (a) Wang, X.-S.; Lascelles, S. F.; Jackson, R. A.; Armes, S. P. *Chem. Commun.* **1999**, 1817. (b) Wang, X.-S.; Jackson, R. A.; Armes, S. P. *Macromolecules* **2000**, *33*, 255. (c) Wang, X.-S.; Armes, S. P. *Macromolecules* **2000**, *33*, 6640.
- (14) (a) Martin, T. J.; Prochazka, K.; Munk, P.; Webber, S. E. *Macromolecules* **1996**, *29*, 6071. (b) Prochazka, K.; Martin, T. J.; Munk, P.; Webber, S. E. *Macromolecules* **1996**, *29*, 6518.
- (15) (a) Gohy, J. F.; Antoun, S.; Jerome, R. *Macromolecules* **2001**, *34*, 7435. (b) Gohy, J. F.; Willet, N.; Varshney, S.; Zhang, J.; Jerome, R. *Angew. Chem., Int. Ed.* **2001**, *40*, 3214.
- (16) (a) Butun, V.; Billingham, N. C.; Armes, S. P. *Chem. Commun.* **1997**, 671. (b) Lee, A. S.; Gast, A. P.; Butun, V.; Armes, S. P. *Macromolecules* **1999**, *32*, 4302. (c) Butun, V.; Armes, S. P.; Billingham, N. C. *Polymer* **2001**, *42*, 5993. (d) Vamvakaki, M.; Billingham, N. C.; Armes, S. P. *Macromolecules* **1999**, *32*, 2088.
- (17) (a) Liu, S.; Billingham, N. C.; Armes, S. P. *Angew. Chem., Int. Ed.* **2001**, *40*, 2328. (b) Liu, S.; Armes, S. P. *Angew. Chem., Int. Ed.* **2002**, *41*, 1413.
- (18) Chu, B. *Laser Light Scattering*; Academic Press: New York, 1974.
- (19) Berne, B. J.; Pecora, R. *Dynamic Light Scattering*; Plenum Press: New York, 1976.
- (20) Zeng, F.; Shen, Y.; Zhu, S.; Pelton, R. *J. Polym. Sci., Part A: Polym. Chem.* **2000**, *38*, 3821.
- (21) Malet, F. L. G. PhD Thesis, University of Sussex, UK, 2001.
- (22) Malet, F. L. G.; Billingham, N. C.; Armes, S. P. To be submitted to *J. Polym. Sci., Part A: Polym. Chem.*
- (23) Zhang, X.; Matyjaszewski, K. *Macromolecules* **1999**, *32*, 1763.
- (24) Matyjaszewski, K.; Shipp, D. A.; McMurtry, G. P.; Gaynor, S. G.; Pakula, J. *J. Polym. Sci., Part A: Polym. Chem.* **2000**, *38*, 2023.
- (25) Liu, S.; Weaver, J. V. M.; Save, M.; Armes, S. P. *Langmuir*, submitted for publication.
- (26) Robinson, K. L.; de Paz-Bañez, M. V.; Wang, X. S.; Armes, S. P. *Macromolecules* **2001**, *34*, 5799.
- (27) Save, M.; Weaver, J. V.; Armes, S. P.; McKenna, P. *Macromolecules* **2002**, *35*, 1152.
- (28) Lobb, E. J.; Ma, I.; Billingham, N. C.; Armes, S. P. *J. Am. Chem. Soc.* **2001**, *123*, 7913.
- (29) McDonald, S.; Rannard, S. P. *Macromolecules* **2001**, *34*, 8600.
- (30) The target degree of quaternization is close (but not identical) to the target degree of cross-linking. This is because the BIEE might react with DMA residues on the same chain; i.e., intrachain quaternization may occur rather than interchain quaternization.
- (31) Mathur, A. M.; Drescher, B.; Scranton, A. B.; Klier, J. *Nature (London)* **1998**, *392*, 367.

MA020447N